# Visible Vectors and Discrete Euclidean Medial Axis

**Jérôme Hulin · Edouard Thiel**

**Abstract** We denote by $\mathcal{M}_R^n$ the test neighbourhood sufficient to extract the Euclidean Medial Axis of any $n$-dimensional discrete shape whose inner radius is no greater than $R$. In this paper, we study properties of discrete Euclidean disks overlappings so as to prove that in any given dimension $n$, $\mathcal{M}_R^n$ tends to the set of visible vectors as $R$ tends to infinity.

**Keywords** Medial axis · Look-up table · Squared Euclidean distance transform ·
Visible points · Disks overlappings

## 1 Introduction

The Medial Axis (MA) is an important tool in image analysis, shape description, computer vision, robot motion planning, surface reconstruction, etc. It provides a global and centred representation of a shape $\mathcal{S}$, a shape being for example a discrete set of points or the frontier of a compact, depending on the considered working space. The medial axis allows one to simplify, compress or compute a reversible skeleton of $\mathcal{S}$. First proposed by Blum in [2], MA was defined in [11] as the set of centres (and radii) of maximal disks in $\mathcal{S}$, a disk being maximal in $\mathcal{S}$ if it is not included in any single other disk included in $\mathcal{S}$. The medial axis is a cover of the input shape, i.e., the union of the balls of MA($\mathcal{S}$) is exactly $\mathcal{S}$, and thus MA is a reversible coding.

J. Hulin · E. Thiel (✉)
Laboratoire d'Informatique Fondamentale de Marseille (LIF, UMR 6166), Université de la
Méditerranée, 163 Av. de Luminy, case 901, 13288 Marseille Cedex 9, France
e-mail: Edouard.Thiel@lif.univ-mrs.fr
url: http://www.lif.univ-mrs.fr/~thiel

J. Hulin
e-mail: Jerome.Hulin@lif.univ-mrs.fr

In this paper, we only consider shapes as bitmaps, i.e., a shape is a subset of $\mathbb{Z}^n$ (without topology considerations). When the disks are distance balls, the MA points can be locally detected on the Distance Transform (DT) of the shape, where each shape point is labelled with the distance to its closest point in the background [16]. Then, a Reverse Distance Transformation (RDT) applied on MA allows one to recover exactly the original shape. Note that a maximal disk can be included in the union of several maximal disks; therefore MA, which is unique by definition, is seldom a minimal cover.

The most important discrete distances used in image analysis for bitmaps (in $\mathbb{Z}^n$) are the squared Euclidean distance $d_E^2$ (squared to store integers) and chamfer distances $d_C$, also known as weighted distances (introduced in [9]). Note that $d_E$ is also denoted $\ell_2$ in the literature and that both $\ell_1$ and $\ell_\infty$ are simple cases of chamfer distances. Chamfer DT and RDT are well known [3, 9, 16] with a simple and fast sequential in two raster scans computation; complexity is $\mathcal{O}(N.m)$, where $N$ is the number of points of the image, and $m$ is the cardinal of the chamfer mask. A number of Squared Euclidean DT algorithms have been proposed over the past 30 years; see for example [12] or the recent one from Hirata [7], which is exact in arbitrary dimension and easily parallelised, with a $\mathcal{O}(N.n)$ time complexity, $n$ being the dimension. The same complexity holds for the computation of the Squared Euclidean RDT [6].

The characterisation of MA is simple for distances such as $\ell_1$, $\ell_\infty$ [16] or $3 \times 3$ chamfer masks [1] by detecting the local maxima on DT, possibly lowering some DT labels before. A general approach using look-up tables (LUT for short) has been introduced for $d_E^2$ in [4] and for a $5 \times 5$ chamfer mask in [5]. The LUT gives for each value read in the DT, the minimum value of the neighbours that forbids a point to be in the MA. The neighbours which are necessary to test for each point of the shape are stored as a set $\mathcal{M}_R^n$ of vectors. The test neighbourhood $\mathcal{M}_R^n$ is sufficiently large to detect the MA of all $n$-dimensional shapes whose inner radii are no greater than $R$, the inner radius of a shape $\mathcal{S}$ being the radius of a largest ball included in $\mathcal{S}$.

The algorithms to compute both LUT and the neighbourhood $\mathcal{M}_R^n$ are given in [15] for $d_E^2$ and [14] for chamfer norms, in any dimension $n$. The extraction of MA from DT using a precomputed $\mathcal{M}_R^n$ and LUT is linear in $N * \text{card}(\mathcal{M}_R^n)$. The computation of the LUT is linear in $N$ for each vector in $\mathcal{M}_R^n$. A fast algorithm to compute the test neighbourhood in the case of 2-dimensional chamfer norms, using the polytope description of discs, is proposed in [10]. The computation of $\mathcal{M}_R^n$ is time consuming in the case of the Euclidean distance, but $\mathcal{M}_R^n$ can be calculated once for all bounded size images and stored at low memory cost (while LUTs can be huge and might be recomputed each time).

Alternative medial axes were recently proposed. In [13], an efficient algorithm, based on [15], computes the Higher Medial Axis (HMA), a medial axis for $d_E^2$ in a doubled resolution grid, which permits the application of further homotopic thinning for the computation of homotopic skeletons. A new linear-time algorithm in [6], inspired by [7], provides the Reduced Medial Axis (RMA) for $d_E^2$; the basic idea is to filter a set of maximal Euclidean paraboloids; while maximal balls and maximal paraboloids coincide in the continuous case, this is not true in the discrete space, and the resulting RMA is generally different from MA.

In the LUT method, experiments in [14, 15] show completely different properties of $\mathcal{M}_R^n$ depending on the distance used. For any given chamfer norm, $\mathcal{M}_R^n$ is bounded

but can have nonvisible vectors (a vector is said to be visible if its coordinates are co-prime). Concerning $d_E^2$, $\mathcal{M}_R^n$ is unbounded; moreover, $\mathcal{M}_R^n$ has only visible vectors, and progressively, all visible vectors seem to appear in $\mathcal{M}_R^n$ when $R$ grows. This is summarised by a conjecture in [15], which claims that $\mathcal{M}_R^n$ tends to the set of visible vectors of $\mathbb{Z}^n$ as $R$ tends to infinity.

In this paper, we are interested to prove the above conjecture. The difficulty lies in the fact that the algorithm in [15] neither explains why a vector might be selected or not for a radius $R$, nor gives information about the order of appearance of vectors in $\mathcal{M}_R^n$. To our knowledge, there is no closed formula for $\mathcal{M}_R^n$ and LUT. Also, intuition might be distorted by geometry in Euclidean space. We have to deal with *discrete* Euclidean disks, with overlappings of smallest or largest disks including or excluding discrete points. In order to insure the existence of points in some situation, we will construct a family of shapes, involving sometimes huge disks. The reader does not need to be fully acquainted with the DT and LUT algorithms, since neither of them play a part in our proof.

After some definitions and recalls in Sect. 2, we tackle the proof in Sect. 3: we show the unicity of $\mathcal{M}_R^n$ for every $R$, then we prove that nonvisible vectors are superfluous, and finally, that all visible vectors are gradually necessary when $R$ grows. We conclude after a discussion in Sect. 4.

## 2 Definitions

### 2.1 The Discrete Space $\mathbb{Z}^n$

In the following, we consider $\mathbb{Z}^n$ both as an $n$-dimensional $\mathbb{Z}$-module (i.e., a discrete vector space) and as its associated affine space; we set $\mathbb{Z}_*^n = \mathbb{Z}^n \setminus \{0\}$. A *shape* $\mathcal{S}$ is a subset of points of $\mathbb{Z}^n$. The complement of $\mathcal{S}$ (also called *background*), denoted by $\overline{\mathcal{S}}$, is $\mathbb{Z}^n \setminus \mathcal{S}$.

In the remainder of the paper, we only consider the Euclidean distance. Given two points $x$, $y$ and a vector $\boldsymbol{v}$ in $\mathbb{Z}^n$, we denote by $d_E(x, y)$ or $xy$ the Euclidean distance between $x$ and $y$, and by $\|\boldsymbol{v}\|$ the Euclidean norm of $\boldsymbol{v}$. We write $(xy)$ for the line in $\mathbb{R}^n$ passing through $x$ and $y$, and $[xy]$ for the line segment in $\mathbb{R}^n$ joining $x$ and $y$. The Cartesian coordinates of $\boldsymbol{v}$ are denoted by $(v_1, \ldots, v_n)$. A vector $\boldsymbol{v} \in \mathbb{Z}^n$ is *visible from the origin* (visible for short) if $\nexists \boldsymbol{u} \in \mathbb{Z}_*^n$ and $\lambda > 1$ such that $\boldsymbol{v} = \lambda \boldsymbol{u}$, or equivalently, if $gcd(v_1, \ldots, v_n) = 1$. The set of all visible vectors of $\mathbb{Z}^n$ is denoted by $\mathcal{V}^n$ (note that $\vec{0}$ is not visible).

We call $\Sigma^n(x)$ the group of axial and diagonal symmetries in $\mathbb{Z}^n$ about centre $x$. For a given $x$, the cardinal of the group is $\#\Sigma^n(x) = 2^n n!$ (which is 8, 48 and 384 for $n = 2$, 3 and 4). A shape $\mathcal{S}$ is said to be *G-symmetrical* if for every $\sigma \in \Sigma^n(O)$, we have $\sigma(\mathcal{S}) = \mathcal{S}$. The *generator* of a set $X \subseteq \mathbb{Z}^n$ (or $\mathbb{R}^n$) is

$$G(X) = \left\{ (x_1, \ldots, x_n) \in X : 0 \leqslant x_n \leqslant x_{n-1} \leqslant \cdots \leqslant x_1 \right\}. \tag{1}$$

Figure 1 shows $G(\mathbb{R}^n)$ for $n = 2$ (an octant) and $n = 3$. A *G-cone* of $\mathbb{Z}^n$ is, by definition, the image of $G(\mathbb{Z}^n)$ by a given symmetry $\sigma$ in $\Sigma^n(O)$.

G($\mathbb{R}^3$)

G($\mathbb{R}^2$)
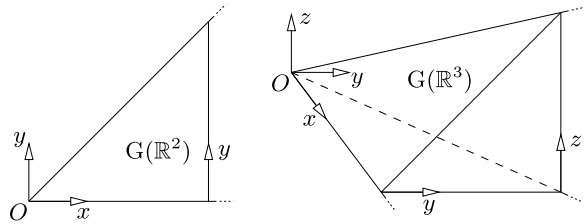
For any set of vectors $\boldsymbol{v}^1, \ldots, \boldsymbol{v}^k \in \mathbb{Z}^n$, $C(\boldsymbol{v}^1, \ldots, \boldsymbol{v}^k)$ stands for the relation: $\boldsymbol{v}^1, \ldots, \boldsymbol{v}^k$ all lie in a common G-cone of $\mathbb{Z}^n$. We also denote by $\neg C(\boldsymbol{v}^1, \ldots, \boldsymbol{v}^k)$ the contrary of the relation $C(\boldsymbol{v}^1, \ldots, \boldsymbol{v}^k)$, i.e., $\exists 1 \leqslant i < j \leqslant k$ such that $\boldsymbol{v}^i$ and $\boldsymbol{v}^j$ do not lie in a same G-cone of $\mathbb{Z}^n$.

Finally, given a vector $\boldsymbol{v} \in \mathbb{Z}^n$, we call $\widetilde{\boldsymbol{v}}$ the *representative* of $\boldsymbol{v}$ in G($\mathbb{Z}^n$), defined to be the vector in G($\mathbb{Z}^n$) verifying $\widetilde{\boldsymbol{v}} = \sigma(\boldsymbol{v})$ for some $\sigma \in \Sigma^n(O)$. According to the definition of the generator (1), $\widetilde{\boldsymbol{v}}$ is unique for any $\boldsymbol{v}$, and its coordinates can be computed by swapping the absolute values of the Cartesian coordinates of $\boldsymbol{v}$ until they are decreasing.

## 2.2 Balls and Medial Axis

The *ball* of centre $x \in \mathbb{Z}^n$ and radius $r \in \mathbb{R}$ is

$$\mathcal{B}(x, r) = \left\{ p \in \mathbb{Z}^n : d_E(x, p) \leqslant r \right\}. \tag{2}$$

Since we consider discrete balls, any ball has an infinite number of radii. We denote by $\sim$ the equivalence relation

$$r \sim r' \quad \Leftrightarrow \quad \mathcal{B}(O, r) = \mathcal{B}(O, r'). \tag{3}$$

The equivalence class of a given $r \in \mathbb{R}$ is the set of all $r' \in \mathbb{R}$ satisfying $\mathcal{B}(O, r) = \mathcal{B}(O, r')$. We define the *representative radius* of a given ball $B$ of centre $x \in \mathbb{Z}^n$ to be the smallest radius $r$ for which $\mathcal{B}(x, r) = B$. As a consequence, the representative radius $r$ is the only radius of its equivalence class for which there exist $a, b \in \mathbb{N}$ such that $r^2 = a^2 + b^2$.

By definition, the considered balls are ascending by inclusion, i.e., such that

$$r \leqslant r' \quad \Rightarrow \quad \mathcal{B}(x, r) \subseteq \mathcal{B}(x, r'). \tag{4}$$

Let $\mathcal{S}$ be a shape and $x \in \mathbb{Z}^n$. We define $I_{\mathcal{S}}(x)$ to be the largest ball of centre $x$ included in $\mathcal{S}$ (if $x \notin \mathcal{S}$, we have $I_{\mathcal{S}}(x) = \emptyset$). Analogously, we denote by $H_{\mathcal{S}}(x)$ the smallest ball of centre $x$ which contains $\mathcal{S}$. See an example in Fig. 2.

The *inner radius* of a given shape $\mathcal{S}$, denoted by rad($\mathcal{S}$), is the representative radius of a largest ball included in $\mathcal{S}$. We denote by CS$^n(R)$ the class of all $n$-dimensional shapes whose inner radii are less than or equal to $R$.

A ball included in $\mathcal{S}$ is called a *maximal ball* of $\mathcal{S}$ if it is not included in any other ball included in $\mathcal{S}$. The *Medial Axis* (MA) of a shape $\mathcal{S}$ is the set of centres (and radii)

**Fig. 2** $H_\mathcal{S}(x)$ and $I_\mathcal{S}(x)$ for a shape $\mathcal{S}$ ($\mathcal{S}$ is represented by bullets)
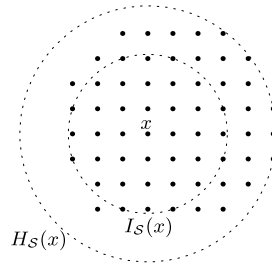


of all maximal balls of $\mathcal{S}$. The balls being ascending by inclusion, we have

$$x \in \mathrm{MA}(\mathcal{S}) \quad \Leftrightarrow \quad x \in \mathcal{S} \text{ and } \forall x' \in \mathcal{S} \setminus \{x\}, I_\mathcal{S}(x) \nsubseteq I_\mathcal{S}(x'). \tag{5}$$

If there exists $\boldsymbol{v} \in \mathbb{Z}_*^n$ such that $I_\mathcal{S}(x) \subseteq I_\mathcal{S}(x - \boldsymbol{v})$, we say that $\boldsymbol{v}$ *forbids* $x$ to be a medial axis point of $\mathcal{S}$.

In order to obtain the radii of all largest balls inside $\mathcal{S}$, we first compute the *Distance Transform* (DT for short) of $\mathcal{S}$ defined by

$$\forall x \in \mathbb{Z}^n, \quad \mathrm{DT}(x) = \min\{d_E^2(x, p) : p \in \overline{\mathcal{S}}\}. \tag{6}$$

Since $d_E^2$ is a discrete distance (i.e., whose values are in $\mathbb{N}$), $\mathrm{DT}(x) - 1$ is a squared radius of the ball $I_\mathcal{S}(x)$. Although MA is computed on the Squared Euclidean Distance Transform (SEDT), which is stored as integer values, the result is actually the MA for $d_E$, since balls of $d_E$ and $d_E^2$ (up to a squared radius) are equivalent.

Compared to the continuous case, no closed formula gives the minimal radius of a discrete ball containing another discrete ball, which is a major difficulty.

## 2.3 Minimum Test Neighbourhood $\mathcal{M}_R^n$

For a given shape $\mathcal{S}$, we need a test neighbourhood $\mathcal{M} \subseteq \mathbb{Z}_*^n$ sufficient to detect, for every $x \in \mathcal{S}$, if $x$ is a point of $\mathrm{MA}(\mathcal{S})$. If $x \notin \mathrm{MA}(\mathcal{S})$, then $\mathcal{M}$ must contain at least one vector $\boldsymbol{v}$ which forbids $x$ to be an MA point. Otherwise, if $x \in \mathrm{MA}(\mathcal{S})$, there is no $\boldsymbol{v} \in \mathbb{Z}^n$ which satisfies $I_\mathcal{S}(x) \subseteq I_\mathcal{S}(x - \boldsymbol{v})$. Thus $\mathcal{M}$ is sufficient for $\mathcal{S}$ iff

$$\forall x \in \mathcal{S}, \quad \big(x \notin \mathrm{MA}(\mathcal{S}) \Rightarrow \exists \boldsymbol{v} \in \mathcal{M}, I_\mathcal{S}(x) \subseteq I_\mathcal{S}(x - \boldsymbol{v})\big). \tag{7}$$

We are interested in computing, for any shape $\mathcal{S}$, a *minimum* test neighbourhood $\mathcal{M}$. More generally, we shall look for a minimum test neighbourhood $\mathcal{M}_R^n$ sufficient to detect the MA of all $n$-dimensional shapes whose inner radii are less than or equal to a given $R$, i.e., shapes in $\mathrm{CS}^n(R)$.

## 3 Properties of the Test Neighbourhood $\mathcal{M}_R^n$

The following observation provides two criterions for excluding a point from the medial axis of a shape, and it will be extensively used in the following proofs. It is a consequence of the fact that the balls are ascending by inclusion, see (4).

**Observation 1** Let $\mathcal{S} \subseteq \mathbb{Z}^n$ be a shape, $x \in \mathcal{S}$, $\boldsymbol{v} \in \mathbb{Z}^n_*$, and let $B = I_{\mathcal{S}}(x)$. The following three sentences are equivalent:

(a) $\boldsymbol{v}$ forbids $x$ to be an MA point of $\mathcal{S}$,
(b) $B \subseteq I_{\mathcal{S}}(x - \boldsymbol{v})$,
(c) $H_B(x - \boldsymbol{v}) \subseteq \mathcal{S}$.

The equivalence $(a) \Leftrightarrow (b)$ is the definition of $\boldsymbol{v}$ forbidding $x$ from MA($\mathcal{S}$). We also clearly have $(c) \Rightarrow (a)$. Finally we have $(b) \Rightarrow (c)$ because $B \subseteq I_{\mathcal{S}}(x - \boldsymbol{v})$ implies that $H_B(x - \boldsymbol{v}) \subseteq I_{\mathcal{S}}(x - \boldsymbol{v})$, and so $B \subseteq H_B(x - \boldsymbol{v}) \subseteq I_{\mathcal{S}}(x - \boldsymbol{v}) \subseteq \mathcal{S}$.

*Remark 1* In figures, we will often represent a discrete ball by the boundary of a continuous counterpart, i.e., a ball in $\mathbb{R}^n$ having an equivalent radius. These figures might seem counter-intuitive, for if a discrete ball is included in another discrete ball, then their continuous counterparts may not satisfy the inclusion.

### 3.1 Unicity of $\mathcal{M}^n_R$

We begin by proving the following proposition:

**Proposition 1** *For all $R \in \mathbb{R}$ and $n \geqslant 2$, there exists a unique test neighbourhood $\mathcal{M}^n_R$ which is minimal by cardinality and sufficient to detect the medial axis of any shape in $\mathrm{CS}^n(R)$.*

*Proof* The existence of $\mathcal{M}^n_R$ is guaranteed by the fact that $\mathbb{Z}^n_*$ is a sufficient test neighbourhood for any $n$-dimensional shape.

Suppose that for given $R \in \mathbb{R}$ and $n \geqslant 2$, there exist two different test neighbourhoods $\mathcal{M}^n_R$ and $\mathcal{M}'^n_R$, both minimal by cardinality. Hence there is at least one vector $\boldsymbol{u}$ in $\mathcal{M}^n_R \setminus \mathcal{M}'^n_R$. Moreover, there exists a shape $\mathcal{S}$ in $\mathrm{CS}^n(R)$ and a point $x$ in $\mathcal{S}$ such that $\boldsymbol{u}$ is the only vector in $\mathcal{M}^n_R$ which forbids $x$ to be in MA($\mathcal{S}$), for otherwise $\boldsymbol{u}$ could be removed from $\mathcal{M}^n_R$, which would contradict the minimality of $\mathcal{M}^n_R$.

We set $B = I_{\mathcal{S}}(x)$ and $H = H_B(x - \boldsymbol{u})$, see Fig. 3. By Observation 1 we have $H \subseteq \mathcal{S}$, so $H \in \mathrm{CS}^n(R)$. Since $\{x - \boldsymbol{u}\}$ is the MA of $H$ (a ball) and $\boldsymbol{u} \notin \mathcal{M}'^n_R$, there exists a vector $\boldsymbol{u}' \neq \boldsymbol{u}$ in $\mathcal{M}'^n_R$ which forbids $x$ to be in MA($H$).

Now, consider $H' = H_B(x - \boldsymbol{u}')$. Since $\boldsymbol{u}'$ forbids $x$ from MA($H$), Observation 1 yields $H' \subseteq H$. Furthermore, $H$ and $H'$ do not coincide, and therefore $H \not\subseteq H'$. Again by Observation 1, it follows that $\boldsymbol{u}$ does not forbid $x$ to be in MA($H'$). In consequence, there exists $\boldsymbol{v} \neq \boldsymbol{u}$ in $\mathcal{M}^n_R$ which forbids $x$ from MA($H'$). However, such a vector $\boldsymbol{v}$ in $\mathcal{M}^n_R$ also forbids $x$ to be in MA($\mathcal{S}$), contradicting the fact that $\boldsymbol{u}$ is the only one. $\qquad\square$

**Corollary 1** *If $0 \leqslant R \leqslant R'$, then $\mathcal{M}^n_R \subseteq \mathcal{M}^n_{R'}$.*

*Proof* By definition, $\mathcal{M}^n_{R'}$ is large enough to detect the MA of any shape in $\mathrm{CS}^n(R)$. Since $\mathcal{M}^n_R$ is unique for every $R$, it follows easily that $\mathcal{M}^n_R \subseteq \mathcal{M}^n_{R'}$. $\qquad\square$

**Fig. 3** A shape $\mathcal{S}$, a ball
$B = I_\mathcal{S}(x)$, and two balls
$H = H_B(x - \boldsymbol{u})$,
$H' = H_B(x - \boldsymbol{u}')$
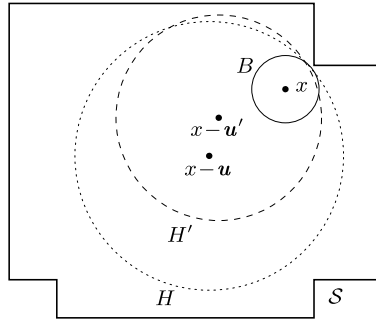
**Corollary 2** *For all $R \geqslant 0$ and $n \geqslant 2$, $\mathcal{M}_R^n$ is G-symmetrical.*

*Proof* By Proposition 1, $\mathrm{G}(\mathcal{M}_R^n)$ is unique. Moreover, the Euclidean balls are G-symmetrical, so $\forall \mathcal{S} \in \mathrm{CS}^n(R), \forall \sigma \in \Sigma^n(O), \sigma(\mathcal{S}) \in \mathrm{CS}^n(R)$. Therefore, $\mathcal{M}_R^n$ is also G-symmetrical. □

We now proceed in two steps in order to prove that $\mathcal{M}_R^n$ tends to $\mathcal{V}^n$ as $R$ tends to infinity. First, we show in Sect. 3.2 that every $\mathcal{M}_R^n$ contains visible vectors only. Second, we show in Sect. 3.3 that for each visible vector $\boldsymbol{v} \in \mathcal{V}^n$, there exists $R \in \mathbb{R}$ such that $\boldsymbol{v}$ belongs to $\mathcal{M}_R^n$.

### 3.2 Nonvisible Vectors Are Superfluous

**Proposition 2** *Let $x$ be a point in a given shape $\mathcal{S} \subseteq \mathbb{Z}^n$, and $\boldsymbol{u}$, $\lambda \boldsymbol{u}$ be two vectors in $\mathbb{Z}_*^n$ with $n \geqslant 2$ and $\lambda > 1$. If $\lambda \boldsymbol{u}$ forbids $x$ to be a point of $\mathrm{MA}(\mathcal{S})$, then so does $\boldsymbol{u}$.*

*Proof* Set $\boldsymbol{v} = \lambda \boldsymbol{u}$, $x' = x - \boldsymbol{u}$, $x'' = x - \boldsymbol{v}$ and $B = I_\mathcal{S}(x)$ (see Fig. 4). Let $p$, $p'$ and $p''$ be points of $B$ (arbitrarily chosen) that maximise the distance to $x$, $x'$ and $x''$, respectively. So we have[1]

$$\forall z \in B, \quad xz \leqslant xp, \qquad x'z \leqslant x'p' \quad \text{and} \quad x''z \leqslant x''p''. \tag{8}$$

Let $B' = \mathcal{B}(x', x'p')$ and $B'' = \mathcal{B}(x'', x''p'')$. By construction, $B' = H_B(x')$ and $B'' = H_B(x'')$.

The hypothesis that $\boldsymbol{v}$ forbids $x$ from $\mathrm{MA}(\mathcal{S})$ is by Observation 1 equivalent to $B \subseteq I_\mathcal{S}(x'')$ or $B'' \subseteq \mathcal{S}$. To prove that $\boldsymbol{u}$ forbids $x$ from $\mathrm{MA}(\mathcal{S})$, we have to show that $B \subseteq I_\mathcal{S}(x')$, or analogously, that $B' \subseteq \mathcal{S}$. It is thus sufficient to show that $B' \subseteq B''$. To complete the proof, we need two preliminary lemmas.

Let $\mathcal{P}$ be the hyperplane in $\mathbb{R}^n$ orthogonal to $\boldsymbol{u}$ and containing $p'$, and let $\mathcal{P}^+$ be the closed half-space delimited by $\mathcal{P}$ and which does not contain $x'$; we have

$$\mathcal{P}^+ = \left\{ z \in \mathbb{R}^n : \boldsymbol{u} \cdot \overrightarrow{p'z} \geqslant 0 \right\}. \tag{9}$$

---

[1] Remember that $ab$ stands for $d_E(a, b)$.

**Fig. 4** $x$, $x'$ and $x''$ are collinear. $\mathcal{S}$ is not shown. The figure may seem counter-intuitive, see Remark 1
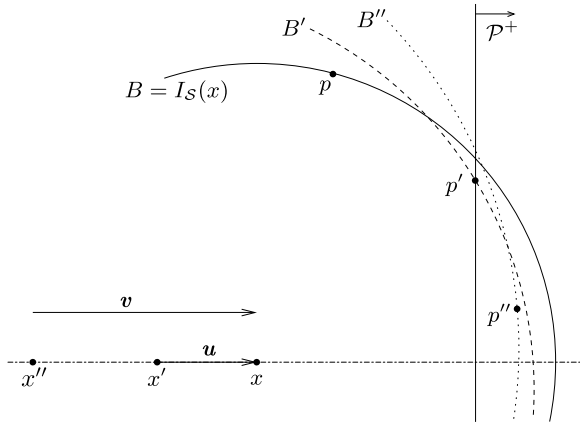


**Lemma 1** *If $z \in B'$ and $z \in \mathcal{P}^+$, then $z \in B$.*

*Proof* Since $z \in B'$, we have $(x'z)^2 \leqslant (x'p')^2$. By inserting $\boldsymbol{u} = \overrightarrow{x'x}$ we obtain $(\boldsymbol{u} + \overrightarrow{xz})^2 \leqslant (\boldsymbol{u} + \overrightarrow{xp'})^2$. Hence $xz^2 + 2\boldsymbol{u} \cdot \overrightarrow{xz} \leqslant xp'^2 + 2\boldsymbol{u} \cdot \overrightarrow{xp'}$, so

$$xz^2 + 2\boldsymbol{u} \cdot \overrightarrow{p'z} \leqslant xp'^2. \tag{10}$$

Since $z \in \mathcal{P}^+$, we have $\boldsymbol{u} \cdot \overrightarrow{p'z} \geqslant 0$ by (9); therefore (10) gives $xz^2 \leqslant xp'^2$, so $xz \leqslant xp'$. Furthermore, $p' \in B$ by definition, so $xp' \leqslant xp$. Thus $xz \leqslant xp$, and so $z \in B$. $\square$

**Lemma 2** *Suppose that $\boldsymbol{v} = \lambda\boldsymbol{u}$ with $1 < \lambda \in \mathbb{R}$. If $z \in B'$ and $z \notin B''$, then $z \in \mathcal{P}^+$.*

*Proof* Since $z \in B'$, we have $x'z \leqslant x'p'$. By inserting $\boldsymbol{u} = \overrightarrow{x'x}$ we can write $(\boldsymbol{u} + \overrightarrow{xz})^2 \leqslant (\boldsymbol{u} + \overrightarrow{xp'})^2$, so

$$xz^2 + 2\boldsymbol{u} \cdot \overrightarrow{xz} \leqslant xp'^2 + 2\boldsymbol{u} \cdot \overrightarrow{xp'}. \tag{11}$$

We also suppose that $z \notin B''$, so $x''p'' < x''z$. Since by definition $p' \in B \subseteq B''$, we have $x''p' \leqslant x''p''$, thus $x''p' < x''z$. By inserting $\boldsymbol{v} = \overrightarrow{x''x}$ we have $(\boldsymbol{v} + \overrightarrow{xp'})^2 < (\boldsymbol{v} + \overrightarrow{xz})^2$, and so

$$xp'^2 + 2\boldsymbol{v} \cdot \overrightarrow{xp'} < xz^2 + 2\boldsymbol{v} \cdot \overrightarrow{xz}. \tag{12}$$

By adding (11) and (12) we obtain $\boldsymbol{u} \cdot \overrightarrow{xz} + \boldsymbol{v} \cdot \overrightarrow{xp'} < \boldsymbol{u} \cdot \overrightarrow{xp'} + \boldsymbol{v} \cdot \overrightarrow{xz}$, and thus $\boldsymbol{u} \cdot \overrightarrow{p'z} < \boldsymbol{v} \cdot \overrightarrow{p'z}$. Provided that $\boldsymbol{v} = \lambda\boldsymbol{u}$, $\lambda > 1$, it follows that $(\lambda - 1)\boldsymbol{u} \cdot \overrightarrow{p'z} > 0$, so $\boldsymbol{u} \cdot \overrightarrow{p'z} > 0$, and thus $z \in \mathcal{P}^+$. $\square$

These two lemmas allow us to complete the proof of Proposition 2; recall that we want to establish the inclusion $B' \subseteq B''$. Suppose that there exists a point $z$ in $B' \setminus B''$. According to Lemma 2, we have $z \in \mathcal{P}^+$. So $z \in B'$ and $z \in \mathcal{P}^+$, and therefore by

Lemma 1 we get $z \in B$. Thus $z \in B$ and $z \notin B''$, but by construction $B \subseteq B''$, a contradiction. $\qquad\square$

**Proposition 3** *No $\mathcal{M}_R^n$ contains nonvisible vectors.*

*Proof* Let $\boldsymbol{u}$ be a visible vector and $\boldsymbol{v} = \lambda\boldsymbol{u}$ with $\lambda \in \mathbb{N}$, $\lambda > 1$. To obtain a contradiction, suppose that there exists a radius $R$ for which $\boldsymbol{v} \in \mathcal{M}_R^n$. According to Proposition 2, $\boldsymbol{v}$ can be replaced with $\boldsymbol{u}$ in $\mathcal{M}_R^n$. If $\boldsymbol{u}$ is already in $\mathcal{M}_R^n$, then $\boldsymbol{v}$ is useless and $\mathcal{M}_R^n$ is not minimal. Else, $\mathcal{M'}_R^n = (\mathcal{M}_R^n \setminus \{\boldsymbol{v}\}) \cup \{\boldsymbol{u}\}$ has the same cardinality as $\mathcal{M}_R^n$, and therefore is another minimal neighbourhood, contradicting unicity in Proposition 1. $\qquad\square$

### 3.3 All Visible Vectors Are Gradually Necessary

We first need three preliminary lemmas. The first two will help defining the so-called candidates of a given visible vector $\boldsymbol{v}$, a set of vectors of *finite cardinality* which will be sufficient to consider when we will prove that $\boldsymbol{v}$ appears in some $\mathcal{M}_R^n$.

**Lemma 3** *Let $\boldsymbol{u}, \boldsymbol{v} \in \mathbb{Z}_*^n$ with $n \geqslant 2$. If $\neg C(\boldsymbol{u},\boldsymbol{v})$, then $\|\boldsymbol{u} + \boldsymbol{v}\| < \|\widetilde{\boldsymbol{u}} + \widetilde{\boldsymbol{v}}\|$.*

*Proof* Without loss of generality, we can assume that $\boldsymbol{u} \in \mathrm{G}(\mathbb{Z}^n)$ and $\boldsymbol{v} \notin \mathrm{G}(\mathbb{Z}^n)$. We define the following transformation $g$:

▷ If $\exists i \leqslant n$ such that $v_i < 0$, then $g(\boldsymbol{v}) = (|v_1|, \ldots, |v_n|)$.
▷ Else, if there exist at least two indexes $i < j \leqslant n$ such that $v_i < v_j$ and $u_i > u_j$, then $g(\boldsymbol{v}) = (v_1, \ldots, v_{i-1}, v_j, v_{i+1}, \ldots, v_{j-1}, v_i, v_{j+1}, \ldots, v_n)$.
▷ Else, we have $\boldsymbol{v} \in \mathrm{G}(\mathbb{Z}^n)$, so we set $g(\boldsymbol{v}) = \boldsymbol{v}$.

All the coordinates of $\boldsymbol{u}$ are positive, so if the first case applies, then clearly $\|\boldsymbol{u} + \boldsymbol{v}\| < \|\boldsymbol{u} + g(\boldsymbol{v})\|$. If the second case applies, then

$$\|\boldsymbol{u} + g(\boldsymbol{v})\|^2 - \|\boldsymbol{u} + \boldsymbol{v}\|^2 = (u_i + v_j)^2 + (u_j + v_i)^2 - (u_i + v_i)^2 - (u_j + v_j)^2$$
$$= 2(u_i - u_j)(v_j - v_i),$$

which is strictly positive. $\widetilde{\boldsymbol{v}}$ is constructed from $\boldsymbol{v}$ by repeated applications of $g$, at least once. Finally we obtain

$$\|\boldsymbol{u} + \boldsymbol{v}\| < \|\boldsymbol{u} + g(\boldsymbol{v})\| < \|\boldsymbol{u} + g(g(\boldsymbol{v}))\| < \cdots < \|\boldsymbol{u} + \widetilde{\boldsymbol{v}}\|. \qquad\square$$

The lemma still holds if we consider three or more vectors, the hypothesis being that at least two of them do not satisfy the relation $C$. The method of proof is unchanged.

**Lemma 4** *Let $\boldsymbol{u}, \boldsymbol{v}$ be two vectors in $\mathbb{Z}_*^n$ and $B$ be a discrete ball of centre $x \in \mathbb{Z}^n$ with $n \geqslant 2$. Let $B' = H_B(x - \boldsymbol{u})$ and $B'' = H_B(x - \boldsymbol{v})$. If $\neg C(\boldsymbol{u}, \boldsymbol{v}, \boldsymbol{v} - \boldsymbol{u})$, then $B' \nsubseteq B''$.*

**Fig. 5** A point $q$ in $B' \setminus B''$. For the sake of clarity, only a quarter of $B$ is drawn (*black bullets*). In general, $z$ may not be equal to $\widetilde{z}$
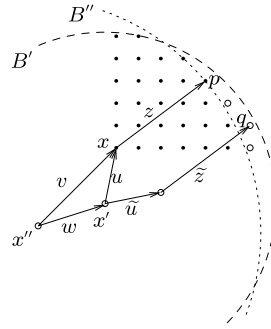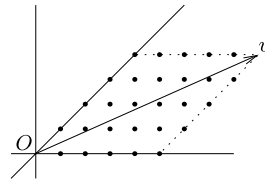


**Fig. 6** The set $\mathcal{A}(v)$ of candidates (represented by *bullets*) of a visible vector $v$



*Proof* The procedure is to find a point $q$ in $B' \setminus B''$. Let $x' = x - u$, $x'' = x - v$, $w = v - u = \overrightarrow{x''x'}$ (see Fig. 5).

Without loss of generality, we can assume that $w \in \mathrm{G}(\mathbb{Z}^n)$. Let $p$ be a point (arbitrarily chosen) of $B$ which maximises its distance to $x''$, and set $z = p - x$. By construction, $x''p = \|v + z\|$ is the representative radius of $B''$. Now consider $q = x' + \widetilde{u} + \widetilde{z}$. We have $x'q = \|\widetilde{u} + \widetilde{z}\|$ and $x''q = \|\overrightarrow{x''x'} + \overrightarrow{x'q}\| = \|w + \widetilde{u} + \widetilde{z}\|$. Let $\sigma$ denote the symmetry in $\Sigma^n(x')$ satisfying $\sigma(u) = \widetilde{u}$, and set $\widetilde{B} = \sigma(B)$. Since $\sigma$ preserves distances, $\widetilde{B} \in B'$. Furthermore, $q \in \widetilde{B}$, so $q \in B'$.

The hypothesis $\neg C(u, v, w)$ implies that $u$ and $w$ do not lie in a common G-cone, for otherwise $v$ would also lie in the same G-cone, since by definition $v = u + w$. So we have $\neg C(w, u)$, and therefore $\|\widetilde{w} + \widetilde{u} + \widetilde{z}\| > \|w + u + z\|$ by extension of Lemma 3 to three vectors.

Since $w \in \mathrm{G}(\mathbb{Z}^n)$, we have $\widetilde{w} = w$, and hence

$$x''q = \|w + \widetilde{u} + \widetilde{z}\| > \|w + u + z\| = x''p.$$

Since $x''p$ is the representative radius of $B''$, we deduce that $q \notin B''$. Consequently, we have proved that $q \in B' \setminus B''$.    □

From now on, we call

$$\mathcal{A}(v) = \left\{ u \in \mathbb{Z}_*^n : u \neq v \text{ and } C(u, v, v - u) \right\} \tag{13}$$

the set of the *candidates* of a given visible vector $v$. Geometrically speaking, the candidates of $v$ are a finite set of vectors which are smaller than $v$ and angularly close to $v$. An example of candidates in the 2-dimensional case is given in Fig. 6.

The following lemma will be central to prove that every visible vector belongs to some $\mathcal{M}_R^n$. Let $B$ be a ball of centre $x$ and radius $r$. If the working space was $\mathbb{R}^n$

instead of $\mathbb{Z}^n$, we would naturally have $\mathrm{rad}(H_B(x - v)) = r + \|v\|$. This is generally false in the discrete space. However, the lemma states that in the discrete space, this equality tends to be satisfied as $r$ tends to infinity.

**Lemma 5** *Let $v$ be a vector in $\mathbb{Z}_*^n$ (with $n \geqslant 2$), $x \in \mathbb{Z}^n$ and $r \in \mathbb{R}_+$. Let $r'$ denote a radius of the smallest discrete ball of centre $x' = x - v$ which contains $\mathcal{B}(x, r)$. Then we have*

$$\lim_{r \to +\infty} r + \|v\| - r' = 0.$$

*Proof* Let $p$ be the farthest point from $x$ included in $\mathcal{B}(x, r)$ verifying $p = x + \lambda v$ for some $\lambda \in \mathbb{N}$ (see Fig. 7). There exists a vector in $\mathbb{Z}^n$ (say $z$) orthogonal to $v$ whose norm is no greater than that of $v$: for instance, take $z = (-v_2, v_1, 0, \ldots, 0)$. Let $q \in \mathbb{Z}^n$ be the farthest point from $p$ included in $\mathcal{B}(x, r)$ which satisfies $q = p + k.z$ for some $k \in \mathbb{Z}_+$; and let $t \in \mathbb{R}^n$ be the point satisfying both $xt = r$ and $t = p + l.z$ for some $l \in \mathbb{R}_+$. We have

$$pq \geqslant pt - \|z\| \geqslant pt - \|v\|. \tag{14}$$

Since $z$ is orthogonal to $v$, we have

$$pt^2 = xt^2 - xp^2 \tag{15}$$

and also

$$r'^2 \geqslant x'q^2 = x'p^2 + pq^2. \tag{16}$$

Substituting (14) and (15) into (16) yields

$$r'^2 \geqslant x'p^2 + \left(\sqrt{xt^2 - xp^2} - \|v\|\right)^2. \tag{17}$$

Replacing $x'p$ by $xp + \|v\|$ and $xt$ by $r$, we can rewrite (17) as

$$
\begin{aligned}
r'^2 &\geqslant \left(xp + \|v\|\right)^2 + \left(\sqrt{r^2 - xp^2} - \|v\|\right)^2 \\
&\geqslant \left(xp + \|v\|\right)^2 + r^2 - xp^2 + v^2 - 2\|v\|\sqrt{r^2 - xp^2} \\
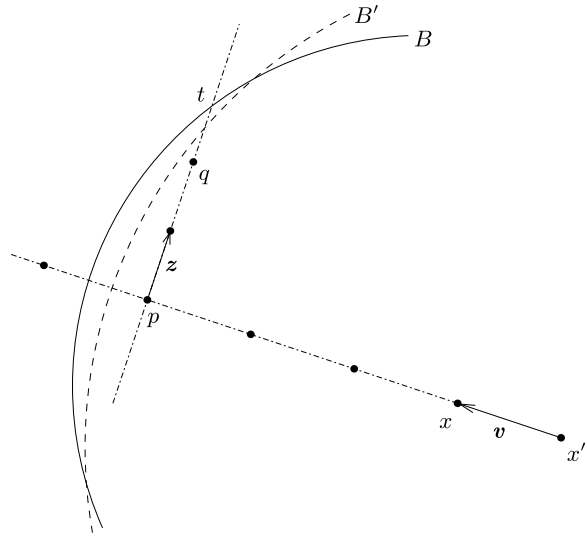&\geqslant \|v\|\left(2xp + \|v\|\right) + r^2 + v^2 - 2\|v\|\sqrt{r^2 - xp^2}.
\end{aligned} \tag{18}
$$

By construction we have $xp > r - \|v\|$, and hence

$$r^2 - xp^2 < r^2 - \left(r - \|v\|\right)^2 < 2\|v\|r.$$

Using the last two inequalities, we can develop (18) into

$$
\begin{aligned}
r'^2 &\geqslant \|v\|\left(2r - \|v\|\right) + r^2 + v^2 - 2\|v\|\sqrt{2\|v\|r} \\
&\geqslant r^2 + 2\|v\|r - 2\|v\|\sqrt{2\|v\|r}.
\end{aligned} \tag{19}
$$

With the notation $\Delta(r) = r + \|\boldsymbol{v}\| - r'$, we deduce from (19) that

$$\Delta(r) \leqslant r + \|\boldsymbol{v}\| - \sqrt{\left(r + \|\boldsymbol{v}\|\right)^2 - 2\|\boldsymbol{v}\|\sqrt{2\|\boldsymbol{v}\|r} - \boldsymbol{v}^2}.$$

A Taylor development at first order of the right-hand side of this expression gives

$$\Delta(r) \leqslant \frac{\|\boldsymbol{v}\| . \sqrt{2\|\boldsymbol{v}\|}}{\sqrt{r}} + o\left(\frac{1}{r}\right) \quad \text{as } r \to +\infty.$$

Consequently, the limit of $\Delta(r)$ is 0 as $r \to +\infty$. □

**Proposition 4** *For all $n \geqslant 2$ and $\boldsymbol{v} \in \mathcal{V}^n$, there exists $R \in \mathbb{R}_+$ such that $\boldsymbol{v} \in \mathcal{M}_R^n$.*

*Proof* Let $\boldsymbol{v}$ be a given visible vector in $\mathcal{V}^n$, and let $x \in \mathbb{Z}^n$. The basic idea of the proof is to construct a shape $\mathcal{S} \subseteq \mathbb{Z}^n$ such that $\boldsymbol{v}$ is the only vector which forbids $x$ to be in the medial axis of $\mathcal{S}$, i.e.,
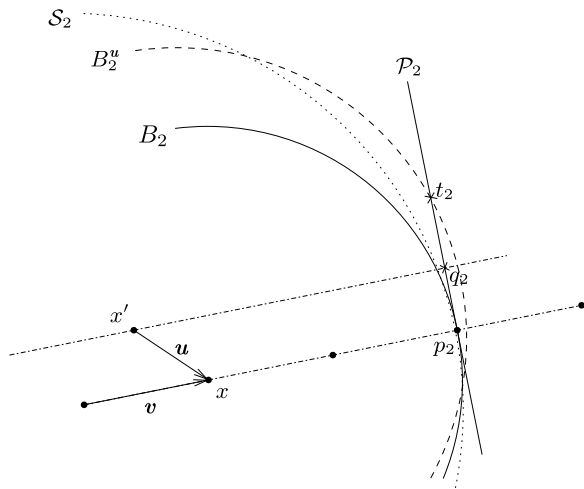
$$\begin{cases} I_{\mathcal{S}}(x) \subseteq I_{\mathcal{S}}(x - \boldsymbol{v}), \\ \forall \boldsymbol{u} \in \mathbb{Z}_*^n \setminus \{\boldsymbol{v}\}, \quad I_{\mathcal{S}}(x) \nsubseteq I_{\mathcal{S}}(x - \boldsymbol{u}). \end{cases} \tag{20}$$

Equivalently, if we consider $B = I_{\mathcal{S}}(x)$, according to Observation 1, we have to show that

$$\begin{cases} H_B(x - \boldsymbol{v}) \subseteq \mathcal{S}, \\ \forall \boldsymbol{u} \in \mathbb{Z}_*^n \setminus \{\boldsymbol{v}\}, \quad H_B(x - \boldsymbol{u}) \nsubseteq \mathcal{S}. \end{cases} \tag{21}$$

For any $k \in \mathbb{N}$, set $p_k = x + k.\boldsymbol{v}$, $B_k = \mathcal{B}(x, k\|\boldsymbol{v}\|)$ and $\mathcal{S}_k = \mathcal{B}(x - \boldsymbol{v}, (k+1)\|\boldsymbol{v}\|)$. An example is given in Fig. 8. Since $\mathrm{rad}(H_{B_k}(x - \boldsymbol{v})) \leqslant \mathrm{rad}(B_k) + \|\boldsymbol{v}\|$ and $p_k \in \mathcal{S}_k$, we have $\mathcal{S}_k = H_{B_k}(x - \boldsymbol{v})$.

**Fig. 8** $B_k$, $B_k^u$, $\mathcal{S}_k$ in the plane $\mathcal{W}(u)$, for $k = 2$



For any $u \in \mathbb{Z}_*^n$, let $B_k^u = H_{B_k}(x - u)$. According to Lemma 4, $\neg C(u, v, v - u)$ implies that $B_k^u \not\subseteq \mathcal{S}_k$, and hence $u$ does not forbid $x$ from $\mathrm{MA}(\mathcal{S}_k)$. Therefore, to complete the proof, we need only consider $\mathcal{A}(v)$ (the candidates of $v$) and find an integer $\gamma$ for which

$$\forall u \in \mathcal{A}(v), \quad B_\gamma^u \not\subseteq \mathcal{S}_\gamma. \tag{22}$$

For any $u \in \mathcal{A}(v)$, let $\mathcal{W}(u)$ denote the 2-dimensional plane in $\mathbb{R}^n$ containing $x$, $v$ and $u$. We also denote by $\mathcal{P}_k$ the hyperplane in $\mathbb{R}^n$ orthogonal to $v$ and which contains $p_k$. By construction, $p_k$ is the only point in $\mathcal{S}_k \cap \mathcal{P}_k$. Set $x' = x - u$, let $q_k$ denote the orthogonal projection of $x'$ onto $\mathcal{P}_k$, and let $t_k$ be the point verifying $x't_k = \mathrm{rad}(B_k^u)$ and $t_k = p_k + \lambda \overrightarrow{p_k q_k}$ for some $\lambda \in \mathbb{R}_+$. Note that in general, $q_k$ and $t_k$ are not points of $\mathbb{Z}^n$. We can write

$$(q_k t_k)^2 = (x't_k)^2 - (x'q_k)^2. \tag{23}$$

By projecting $u$ onto $v$ we can rewrite $x'q_k$ as $xp_k + \|u\| \cos(u, v)$, and hence

$$(q_k t_k)^2 = (x't_k)^2 - \big(xp_k + \|u\| \cos(u, v)\big)^2$$
$$= \big(x't_k + xp_k + \|u\| \cos(u, v)\big)\big(x't_k - xp_k - \|u\| \cos(u, v)\big). \tag{24}$$

Since $xp_k$ and $x't_k$ are the radii of $B_k$ and $B_k^u$ respectively, Lemma 5 shows that

$$\lim_{k \to +\infty} x't_k - xp_k = \|u\|. \tag{25}$$

Since $u \in \mathcal{A}(v)$, the vectors $u$ and $v$ are not collinear with each other, and $0 < \cos(u, v) < 1$. So, combining (24) and (25), we deduce that

$$\lim_{k \to +\infty} q_k t_k = +\infty. \tag{26}$$

Each line $(p_k q_k)$ passes through infinitely many points of $\mathbb{Z}^n$, because $p_k \in \mathbb{Z}^n$ and there exists at least one discrete vector $z \in \mathcal{W}(u) \cap \mathcal{P}_k$, for example, take $z = (u \wedge$

$v) \wedge v$. Moreover, the integer points on the line segment $[q_k t_k]$ are in $B_k^u \setminus S_k$ since $[q_k t_k] \subseteq \mathcal{P}_k$ and $\mathcal{P}_k \cap S_k = p_k$. On account of (26) and the above remarks, it follows that

$$\forall u \in \mathcal{A}(v), \ \exists k_u \in \mathbb{N}, \ \forall k > k_u, \quad B_k^u \nsubseteq S_k. \tag{27}$$

Finally, we see that taking $\gamma = \max\{k_u : u \in \mathcal{A}(v)\}$ is sufficient to satisfy (22). The existence of $\gamma$ is ensured by the fact that $\mathcal{A}(v)$ is bounded for every $v$. $\qquad\square$

We can now formulate our main result. By Propositions 3 and 4, we have shown the following:

**Theorem 1** *The minimum test neighbourhood $\mathcal{M}_R^n$ sufficient to detect the discrete Euclidean medial axis of any shape in $\mathrm{CS}^n(R)$ satisfies $\lim_{R \to +\infty} \mathcal{M}_R^n = \mathcal{V}^n$.*

## 4 Discussion

### 4.1 On the Density of $\mathcal{V}^n$

Let $v$ be a vector in $\mathbb{Z}^n$, selected at random. The probability $p(n)$ that $v$ is visible is given by $\frac{1}{\zeta(n)}$ (see [8]), where $\zeta(n)$ is the Riemann zeta function defined for any integer $n$ by

$$\zeta(n) = \sum_{k=1}^{+\infty} \frac{1}{k^n}.$$

For the two-dimensional case, this gives

$$p(2) = \frac{1}{\zeta(2)} = \frac{6}{\pi^2} \approx 0.61.$$

In higher dimensions we have $p(3) \approx 0.83$ and $p(4) \approx 0.92$. Moreover, $p(n)$ grows with $n$ and tends to 1 as $n \to +\infty$. So we see that the probability that a point (selected at random) belongs to some $\mathcal{M}_R^n$ is quite high.

### 4.2 On the Appearance Radii

The *appearance radius* of a given vector $v \in \mathcal{V}^n$, denoted by $R(v)$, is defined to be the smallest Euclidean radius $R \in \mathbb{R}$ satisfying $v \in \mathcal{M}_R^n$. We have seen above that $\mathcal{V}^n$ is quite dense in $\mathbb{Z}^n$; however experiments in [15] show that the appearance radius of a given vector $v$ is much greater than the Euclidean norm of $v$. For example, in the 2-dimensional case, it seems that the appearance radius of a given vector $v$ is always greater than the squared norm of $v$.

Future work will be focused on bounding $R(v)$ or $\mathrm{card}(\mathcal{M}_R^n)$. For instance, for a given dimension $n$, if there exists a function $f$ such that $\|v\| \leqslant f(R(v))$ for all $v \in \mathcal{V}^n$, then the set of all visible vectors whose norm is no greater than $f(R)$ will be a sufficient test neighbourhood to detect the medial axis of any $S \in \mathrm{CS}^n(R)$. This way, it will not be necessary to precalculate $\mathcal{M}_R^n$ before extracting the medial axis.

## 5 Conclusion

In this paper, we have established a relation between the set of visible vectors $\mathcal{V}^n$ and the minimum test neighbourhood $\mathcal{M}_R^n$ able to detect the discrete Euclidean medial axis of any shape in $\mathbb{Z}^n$ whose inner radius is no greater than $R$.

The property that nonvisible vectors are superfluous allows one to speed up the computation of $\mathcal{M}_R^n$. The fact that $\mathcal{M}_R^n$ is unbounded when $R$ grows is specific to the Euclidean distance and seems to be false for all chamfer distances. This must be linked to the fact that the discrete Euclidean balls may have an indefinitely large number of faces, whereas the balls of a given chamfer distance are polyhedra with a constant number of faces.

In future works, we hope to improve the characterisation of $\mathcal{M}_R^n$. In particular, we would like to find a lower bound for the appearance radius of any given visible vector. We are also interested in reducing the set of candidates of a given visible vector $\boldsymbol{v}$ (a set of vectors sufficient to consider when computing the appearance radius of $\boldsymbol{v}$), so as to improve the computation complexity of $\mathcal{M}_R^n$.

## References

1. Arcelli, C., Sanniti di Baja, G.: Finding local maxima in a pseudo-Euclidean distance transform. Comput. Vis. Graph. Image Process. **43**, 361–367 (1988)
2. Blum, H.: A transformation for extracting new descriptors of shape. In: Wathen-Dunn, W. (ed.) Models for the Perception of Speech and Visual Form, pp. 362–380. MIT Press, Cambridge (1967)
3. Borgefors, G.: Distance transformations in arbitrary dimensions. Comput. Vis. Graph. Image Process. **27**, 321–345 (1984)
4. Borgefors, G., Ragnemalm, I., Sanniti di Baja, G.: The Euclidean distance transform: finding the local maxima and reconstructing the shape. In: 7th Scandinavian Conf. on Image Analysis, vol. 2, pp. 974–981. Aalborg, Denmark (1991)
5. Borgefors, G.: Centres of maximal disks in the 5–7–11 distance transform. In: 8th Scandinavian Conf. on Image Analysis, pp. 105–111. Tromsø, Norway (1993)
6. Coeurjolly, D.: $d$-Dimensional reverse Euclidean distance transformation and Euclidean medial axis extraction in optimal time. In: 11th DGCI, Naples, Italy, November 2003. Lecture Notes in Computer Sience, vol. 2886, pp. 327–337. Springer, Berlin (2003)
7. Hirata, T.: A unified linear-time algorithm for computing distance maps. Inf. Process. Lett. **58**(3), 129–133 (1996)
8. http://mathworld.wolfram.com/VisiblePoint.html
9. Montanari, U.: A method for obtaining skeletons using a quasi-euclidean distance. J. ACM **15**, 600–624 (1968)
10. Normand, N., Évenou, P.: Medial axis LUT computation for chamfer norms using H-polytopes. In: 14th Discrete Geometry for Computer Imagery, Lyon, France, April 2008. Lecture Notes in Computer Sience, vol. 4992, pp. 189–200. Springer, Berlin (2008)
11. Pfaltz, J.L., Rosenfeld, A.: Computer representation of planar regions by their skeletons. Commun. ACM **10**, 119–125 (1967)
12. Saito, T., Toriwaki, J.I.: New algorithms for Euclidean distance transformation of an $n$-dimensional digitized picture with applications. Pattern Recogn. **27**(11), 1551–1565 (1994)
13. Saúde, A.V., Couprie, M., Lotufo, R.: Exact Euclidean medial axis in higher resolution. In: 13th Discrete Geometry for Computer Imagery, Szeged, Hungary, October 2006. Lecture Notes in Computer Sience, vol. 4245, pp. 605–616. Springer, Berlin (2006)
14. Rémy, E., Thiel, E.: Medial axis for chamfer distances: computing LUT and neighbourhoods in 2D or 3D. Pattern Recogn. Lett. **23**(6), 649–661 (2002)
15. Rémy, E., Thiel, E.: Exact medial axis with Euclidean distance. Image Vis. Comput. **23**(2), 167–175 (2005)
16. Rosenfeld, A., Pfaltz, J.L.: Sequential operations in digital picture processing. J. ACM **13**(4), 471–494 (1966)